

## Self-gated cardiac Cine MRI of the rat on a clinical 3T MRI system

Martin Krämer<sup>1</sup>, Karl-Heinz Herrmann<sup>1</sup>, Judith Biermann<sup>1</sup>, Sebastian Freiburger<sup>2</sup>, Michael Schwarzer<sup>2</sup>, and Jürgen R Reichenbach<sup>1</sup>

<sup>1</sup>Medical Physics Group, Institute of Diagnostic and Interventional Radiology I, Jena University Hospital - Friedrich Schiller University Jena, Jena, TH, Germany,

<sup>2</sup>Department of Cardiothoracic Surgery, Jena University Hospital - Friedrich Schiller University Jena, TH, Germany

**Target Audience** – Researchers using radial trajectories for cardiac imaging and researchers using animal models for investigation of cardiac diseases.

**Purpose** – The ability to perform small animal functional cardiac imaging on clinical MRI scanners may be beneficial when no dedicated high field animal MRI scanner is available. Using clinical MR systems for this purpose is challenging since clinical scanners have lower field strengths and inferior gradient performance<sup>1</sup>. Here, we propose radial MR cardiac imaging in the rat in combination with interspersed navigators for self-gating without any additional external triggering requirements for electrocardiogram (ECG) and respiration on a whole-body clinical 3 T scanner.

**Methods** – To obtain scout overview images for defining the position of the imaged cardiac slices, a multi-slice golden-angle<sup>2</sup> radial sequence was implemented in ODIN<sup>3</sup>. Due to the increased repetition time (TR) of the multi-slice scheme an increased Ernst angle could be used, providing improved SNR. The radial data were merged by 2D gridding with no cardiac and respiratory gating. To increase image contrast radial readouts were acquired with center-in ordering, thus increasing flow sensitivity. All localizer images were reconstructed online using the image reconstruction system of the scanner.

For dynamic cine imaging of the rat heart a single slice, golden-ratio<sup>2</sup> radial sequence was used. Radial readouts were acquired with center-out ordering to achieve in-plane flow compensation. 1D navigator readouts of the measurement slice with the same fixed rotation angle were periodically interleaved with the golden-angle acquisition<sup>4</sup> and used for retrospective gating of the continuously acquired radial data. Navigators were interspersed with a high frequency of 54 Hz (Fig. 1). The correlation function derived from these navigator data was manually thresholded to exclude data acquired during respiratory motion. Peaks in the correlation function passing the threshold were used for selecting small data windows that included 4 measurement spokes. For cine reconstruction a sliding-window approach was used that shifted the data windows by one TR.

All images were acquired on a 3T clinical scanner (TIM Trio, Siemens Healthcare) using an 8 channel CPC multifunctional coil (NORAS MRI products GmbH)<sup>5</sup>. The coil consists of two arrays with 4 channels each, mounted on a flexible holder (Fig. 1). Experiments were performed on 6 healthy female rats (Sprague Dawley, 14 weeks), anesthetized with a mixture of 1.7% isoflurane and O<sub>2</sub>. Localizer images were acquired with parameters: FOV 50 x 50 mm<sup>2</sup>, matrix 144 x 144, 233 radial readouts, TE 4.5 ms, TR 106 ms, 24° FA, 54 kHz BW, 12 slices with no gap. Short axis (and partial 4 chamber) cardiac cine images were acquired using: FOV 50 x 50 mm<sup>2</sup> (55 x 55 mm<sup>2</sup>), matrix 240 x 240, 1.0 mm slice thickness, 754 radial readouts and 377 navigator readouts per *k*-space, TE 2.1 ms, TR 6.5 ms, 10 FA, 51 kHz BW, 60 (80) repetitions and TA 7.3 min (9.8 min).

**Results** – Reconstructed radial localizer images are shown in Figure 2. Although data were averaged with no gating the anatomy of the heart is visible without any major artifacts. The localizer images are dominated by the diastolic motion phase with dark blood contrast caused by the flow sensitive center-in readout. In the navigator correlation time course both the slower respiratory (40 min<sup>-1</sup>) and the high frequency cardiac motions (285 min<sup>-1</sup>) are clearly distinguishable (Fig. 3a). Applying a threshold data acquired during respiratory motion were identified and discarded. Comparing the navigator time course with the signal from a small animal monitoring unit (Fig. 3b) revealed excellent agreement with respect to shape and position of the cardiac peaks. Figure 4a shows cine images for a short axis view with high in-plane (210 x 210 μm<sup>2</sup>) and temporal (6.5 ms) resolution. No artifacts due to cardiac motion are visible, while jet artifacts signify accelerated flow during ventricular blood ejection. Images of a cardiac cine measurement showing left atrium and ventricle as well as the outflow tract of the left ventricle are displayed in Figure 4b.

**Discussion & Conclusion** – High quality cine images were obtained on a clinical 3T system in less than 10 minutes with high temporal and spatial resolutions. Applying center-out trajectories minimized flow artifacts while maintaining visibility of accelerated flow jets. Applying a threshold to exclude respiration contaminated data worked out very well, most likely due to the prone position of the rats, that leads to short respiration followed by long motion free phases. In combination with the continuous golden-angle radial acquisition a high data sampling efficiency was achieved where only 20% to 30% of non-navigator data had to be discarded due to respiratory motion. Due to the retrospective self-gating and the continuous golden-angle acquisition measurement parameters can be individually adjusted to the actual measurement situation. The localizer images acquired with no gating provided sufficient image quality to serve as planning images. The multifunctional CPC coil proved to be well suited for the cardiac measurements. It should, however, be noted that the presented animal setup and acquisition scheme is not limited to this particular coil but can also be performed with a small surface coil or loop coils.

**References** – [1] Herrmann KH, et al., Magn Reson Mater Phy, 2012, 25:233–244 [2] Winkelmann S, et al., IEEE T Med Imaging 2007;26:68–76. [3] Jochimson TH, et al., J Magn Reson, 2004; 170:76-7 [4] Krämer M, et al., J Magn Reson Imaging, 2013; Epub ahead of print [5] Gareis D, et al, 2006, ISMRM #2585#

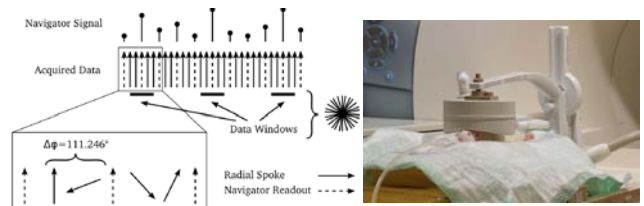


**Fig.1.** Schematic illustration of the acquisition scheme (left) and measurement setup of a rat in a clinical 3T MRI system showing the top module of the CPC coil (right).

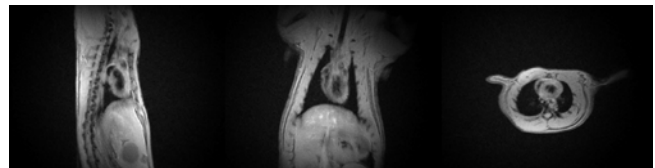


**Fig.2.** Selected slices of the radial localizer images which were used to plan the imaging planes of the cardiac cine acquisition. From left to right images were acquired using sagittal, coronal and transversal orientations of the measurement slice. Images were reconstructed without any gating of the cardiac or respiratory motion, thereby averaging data over different cardiac cycles.

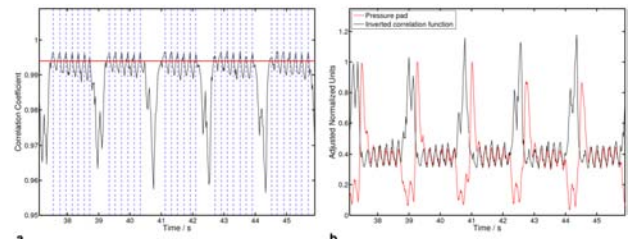


**Fig.3.** (a) Part of the navigator correlation function of a cardiac short axis measurement used for retrospective triggering. Free breathing threshold and trigger points are delineated as red and blue lines, respectively. (b) Overlay of the inverted correlation function with the signal from the pressure pad a small animal monitoring unit.

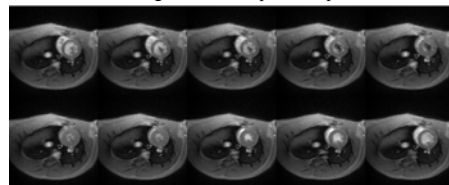


**Fig.4.** (a) Every third frame of short axis cardiac cine images of a rat with 0.21 x 0.21 x 1.00 mm<sup>3</sup> resolution (b) Every second frame of partial 4 chamber view with 0.23 x 0.23 x 1.00 mm<sup>3</sup> resolution.

